JACS
JOURNAL OF THE AMERICAN CHEMICAL SOCIETY
Article
pubs.acs.org/JACS

Size as a Parameter to Stabilize New Phases: Rock Salt Phases of $Pb_mSb_{2n}Se_{m+3n}$

Ronald B. Soriano,[†] Jinsong Wu,[‡] and Mercouri G. Kanatzidis*[,†]

[†]Department of Chemistry and [‡]Department of Material Science, Northwestern University, Evanston, Illinois 60208 United States

Supporting Information

ABSTRACT: A series of $Pb_mSb_{2n}Se_{m+3n}$ nanocrystals (m = 2, 4, 6 and 8; n = 1) are demonstrated that exist only as a distinct phase on the nanoscale. The nanocrystals aggregates are new compounds adopting the cubic NaCl-type structure. These materials form aggregates comprised of nanocrystallites that are attached at a preferred orientation. Elemental compositions were studied using the complementary techniques of scanning transmission electron microscopy/energy dispersive X-ray spectroscopy and inductively coupled plasma-atomic emission spectroscopy. The new ternary nanocrystal aggregates are moderately monodisperse and exhibit well-defined band gap energies in the mid-IR region. The $Pb_mSb_{2n}Se_{m+3n}$ nanomaterials behave as homogeneous solid solutions with lattice parameter trending as a function of Sb incorporation at room temperature and tend to phase separate into PbSe and Sb_2Se_3 at 400 °C.

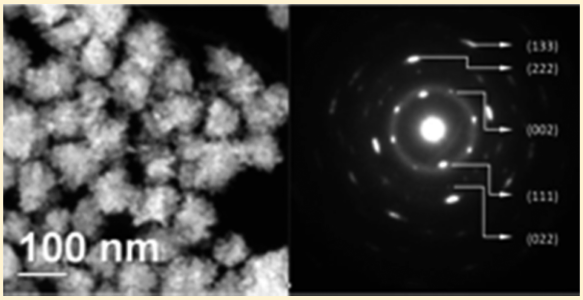

INTRODUCTION

Semiconductor nanocrystals have highly tunable electronic, catalytic, and optical properties through size shape and composition adjustments.[1−7] These unique characteristics make them suitable for various applications such as light emitting diodes,[8−12] optical elements,[13−15] photodetectors,[16−18] solar cells,[19−22] and thermoelectric devices.[23−26] Among the IV−VI semiconductors, the narrow band gap and large Bohr radius of the lead chalcogenide, PbQ (Q = S, Se, and Te) nanocrystals are highly studied infrared quantum dots.[27−29] The rock-salt lattice leads to an electronic band structure different from that of the typical II−VI compounds (e.g., CdQ) with important consequences for the optical and electrical properties in the regime of strong confinement.[30,31] In particular, PbSe has been extensively investigated due to its excellent electronic and optical properties: (1) high absorption coefficient,[32] (2) large Bohr exciton radius (α_B = 46 nm),[30] and (3) high dielectric constant (ε = 24).[33] In addition, PbSe NCs exhibit multiexciton generation (MEG) property that could potentially increase the theoretical efficiency of photovoltaic devices to as high as 43%.[19,34] Sb_2Se_3, a pnicogen chalcogenide (V−VI) binary semiconductor crystallizes in an orthorhombic space group with a highly anisotropic structure.[35,36] It has medium band gap (~1 eV),[37] high Seebeck coefficient,[38] and fast amorphous-to-crystalline phase transition.[39] Because of these attractive electronic and optical properties and good chemical stability it is a potential candidate for photovoltaic, thermoelectric, and electrochemical hydrogen storage applications.[40,41]

Most efforts to date explored the dimensional regime of nanomaterials and its effects on physical properties but little attention have been paid to the possibility of using it as a tool to discover new materials. Recently, our group prepared $Pb_mSb_{2n}Te_{m+3n}$ nanocrystals, which are new phases within the PbTe-Sb_2Te_3 system stabilized in the nanoscale regime.[42] Nonequilibrium phases of oxides (wurtzite-type CoO,[43] $Ni_{1-x}Fe_xCO$[44] and bixbyite V_2O_3)[45] and intermetallic compounds[46,47] [Au_3M[46] and Au_3M_{1-x}[47] (Fe, Co, Ni)] have also been prepared through size reduction to the nanoscale. This represents a new approach to nanoparticle science that has the potential to lead to entirely novel nanomaterials since it is not based on the familiar paradigm of nanosizing known bulk solids. As shown previously, more complex ternary and quaternary nanocrystals can exhibit different properties or enhanced ability for functionalization as demonstrated by the new magnetic properties, higher thermoelectric figure of merit, and the observation of band inversion reported for certain systems.[48−50] Examples of these more complex nanocrystals are the Cu and Ag-chalcogenides which include $CuInS_2$,[51] $CuInSe_2$,[52] Cu_2ZnSnS_4,[53,54] $Cu_2ZnSnSe_4$,[6,55] $AgInS_2$,[51] $AgInSe_2$,[51] and $AgPb_mSbTe_{m+2}$.[48,50]

In this paper we report the preparation of a series of $Pb_mSb_{2n}Se_{m+3n}$ flower-like nanocrystal aggregates with cubic rock-salt type structure ($Fm\bar{3}m$). This family appears to exist only as nanoscale stabilized phase. Based on the bulk phase diagram (Figure 1), only one compound exists in the PbSe-Sb_2Se_3 system and crystallizes in the orthorhombic ($Pnnm$) space group.[56] Further, we confirm that the nanocrystal aggregates are homogeneous (i.e., single phases) as opposed to phase-separated systems.

Received: May 29, 2015
Published: July 16, 2015

DOI: 10.1021/jacs.5b05562
J. Am. Chem. Soc. 2015, 137, 9937−9942

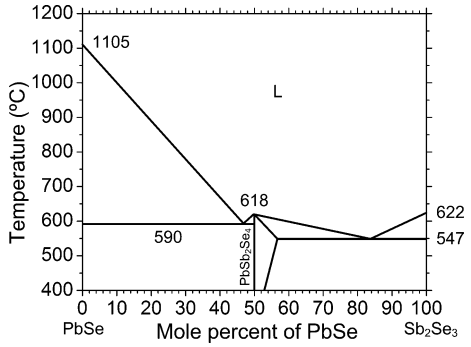

Figure 1. Schematic of the pseudo binary phase diagram of PbSe–Sb_2Se_3 showing the immiscibility of the two phases.

EXPERIMENTAL SECTION

For the materials, synthesis of $Pb_mSb_{2n}Se_{m+3n}$ nanocrystals, and characterization subsections, please refer to the Supporting Information (SI) for detailed descriptions.

RESULTS AND DISCUSSION

The series of $Pb_mSb_{2n}Se_{m+3n}$ nanocrystals was synthesized by a colloidal hot injection method using oleic acid (OA) as surfactant and octadecene (ODE) as the reaction medium. This surfactant/solvent combination, along with lead and antimony acetate salts, has been shown to yield stable, monodisperse and ternary $Pb_mSb_{2n}Te_{m+3n}$ nanocrystals (m = 2, 3, 4, 6, 8 and 10; n = 1 and 2). Elemental Se dissolved in tri-*n*-octyl phosphine (TOP) was used as the Se source. In a synthesis of $Pb_mSb_{2n}Se_{m+3n}$ nanocrystals, acetate salt precursors were converted to oleate salts upon heating the reaction mixture to 100 °C. This subsequent conversion is accompanied by drying to ensure the complete removal of water as the reaction mixture is heated under vacuum. A schematic representation of the synthesis is provided in Figure 2. Complete drying was signaled by the formation of a colorless mixture. The temperature of the resulting solution was raised to 180 °C, and the prepared Se precursor solution was swiftly injected. This temperature is above the decomposition temperature for both antimony and lead oleates. The reaction was allowed to proceed for 2 min to ensure the formation of relatively monodisperse nanocrystal aggregates. The amount of Sb incorporation into the PbSe lattice is close to the nominal amount of the Sb precursor. This suggests that good control of the composition can be achieved by just varying the nominal amounts of the starting precursor.

It is remarkable that a significant amount of Sb can be incorporated into the lattice by using OA as capping ligand, contrary to the previously prepared $Pb_mSb_{2n}Te_{m+3n}$ nanocrystal analogues which require oleylamine in addition to OA in order to stabilize Sb into the PbTe lattice.[42] A possible explanation for the ease of Sb incorporation into the PbSe matrix could be the smaller size difference between Sb and Se.

Powder X-ray diffraction (PXRD) patterns of the prepared $Pb_mSb_{2n}Se_{m+3n}$ nanocrystals exhibit broad diffraction peaks which could be indexed to cubic rock-salt ($Fm\bar{3}m$) symmetry (Figure 3a). No impurity peaks corresponding to binary Sb_2Se_3

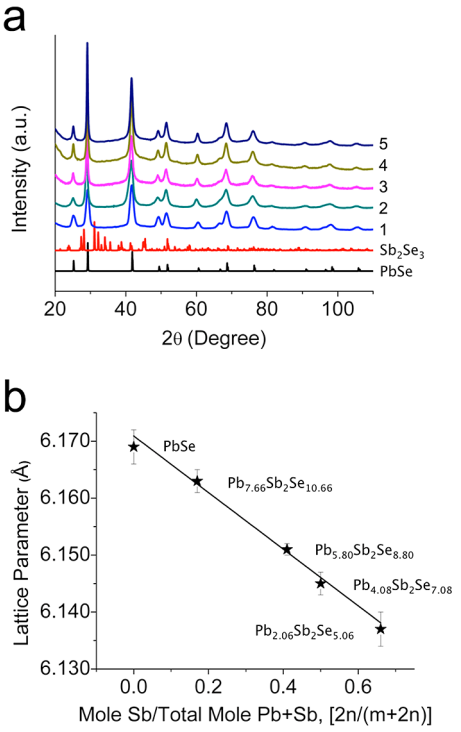

Figure 3. (a) PXRD patterns of (1) PbSe, (2) $Pb_{7.66}Sb_2Se_{10.66}$, (3) $Pb_{5.80}Sb_2Se_{8.80}$, (4) $Pb_{4.08}Sb_2Se_{7.08}$, and (5) $Pb_{2.06}Sb_2Se_{5.06}$ nanocrystal aggregates. Black and red lines represent the simulated PXRD patterns of bulk PbSe (ICSD 648518) and bulk Sb_2Se3 (ICSD 171569), respectively. (b) Change in lattice parameter as a function of increasing Sb incorporation obeys Vegard's law.

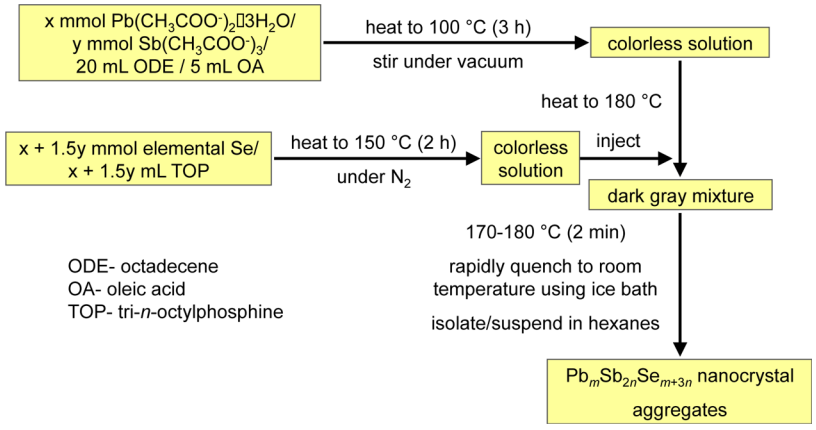

Figure 2. Schematic diagram for the synthesis of the $Pb_mSb_{2n}Se_{m+3n}$ nanocrystals.

DOI: 10.1021/jacs.5b05562
J. Am. Chem. Soc. 2015, 137, 9937–9942

or elemental Pb, Sb, and Se were observed, indicating the single phase nature of the prepared nanoparticles. The diffraction patterns are shifted to larger 2θ values relative to that of PbSe indicating a contracted lattice and confirming the Sb incorporation in the structure. The lattice parameters of $Pb_mSb_{2n}Se_{m+3n}$ nanocrystals decrease systematically with increasing Sb concentration. The samples follow Vegard's law as indicated by a nearly linear relationship when the calculated lattice parameter is plotted against Sb mole fraction (lattice parameter (Å) vs mole Sb/total mole Sb +Pb $[2n/(m+2n)]$) (Figure 3b).

Inductively coupled plasma-atomic emission spectroscopy (ICP-AES) was used to determine the elemental composition of the prepared series of $Pb_mSb_{2n}Se_{m+3n}$ nanocrystals. Prior to ICP-AES analysis, samples were dissolved in *aqua regia*. Complete dissolution was achieved by removal of capping ligands. The presence of capping ligands would have prevented this, as polymerization of capping ligands could be promoted by the presence of *aqua regia* forming rubber-like lumps. Only Pb^{2+} and Sb^{3+} were analyzed as Se is liberated as H_2Se gas during the dissolution process in *aqua regia*. The reported amounts of Se are only estimated, assuming charge-balanced compositions. Energy dispersive spectroscopy attached to a scanning transmission electron microscope (STEM/EDS) was also used as complementary technique to estimate the concentration of Se. From this analysis, a trend in Se concentration can be deduced which is consistent with the estimated Se concentration for charge-balanced particles. The determined actual compositions are very close to the nominal ones further confirming that good control of composition can be achieved by the chosen reaction conditions (Table 1).

Table 1. Elemental Composition, Average Crystallite and Aggregate Size, and Lattice Parameters

		average size (nm)		
nominal composition	actual composition (ICP-AES)	crystallite (PXRD)	aggregate (TEM)	lattice parameters (Å)
$Pb_2Sb_2Se_5$	$Pb_{2.06}Sb_2Se_{5.06}$	14.7	83.0 ± 3.0	6.137(3)
$Pb_4Sb_2Se_7$	$Pb_{4.08}Sb_2Se_{7.08}$	13.9	86.0 ± 2.0	6.145(2)
$Pb_6Sb_2Se_9$	$Pb_{5.80}Sb_2Se_{8.80}$	15.2	91.0 ± 5.0	6.151(1)
$Pb_8Sb_2Se_{11}$	$Pb_{7.66}Sb_2Se_{10.66}$	14.4	89.0 ± 3.0	6.163(2)
PbSe	–	18.6	19.1 ± 0.5	6.169(3)

Contrary to the $Pb_mSb_{2n}Te_{m+3n}$ nanocrystals where control of composition is a challenge,[42] compositions with equal Sb and Pb fractions can be easily prepared. The fact that any member of the $Pb_mSb_{2n}Se_{m+3n}$ family can be prepared in the NaCl structure is remarkable because the total number of metals (Pb + Sb) is less than the number of nonmetals (Se). The higher the Sb fraction the higher the number of vacancies that must be accommodated in the lattice. For example, the $Pb_{2.06}Sb_2Se_{5.06}$ nanocrystal composition must contain a remarkably high fraction of 20% vacancies in the Na site of the rock-salt lattice.

Transmission electron microscopy (TEM) images of $Pb_mSb_{2n}Se_{m+3n}$ nanocrystals are shown in Figure 4a–d. The as-synthesized nanocrystals exhibit flower-like aggregate morphology. The average particle size of the aggregates is ~85 nm. High-resolution TEM showed these aggregates were made up of smaller crystallites ~14.5 nm, consistent with the calculated particle size based on the broadening of the Bragg peaks using the Scherrer equation (Figure 4e). These results are tabulated in Table 1. The same reaction condition used to prepare pure PbSe yielded star-shaped nanocrystals rather than aggregates, consistent with the previously reported role of acetate in the formation of the said morphology (Figure S1).[57] Selected-area electron diffraction (SAED) patterns collected from ~200 × 200 nm area loaded with nanocrystal aggregates further confirm the crystalline nature and display Bragg reflections which could be indexed to a cubic rock-salt ($Fm\bar{3}m$) space group (Figure S2). However, if SAED is done on an individual particle, Bragg reflections spots defining an apparent single crystal pattern are observed indicating that the aggregation is happening at a strongly preferred orientation (Figure 4f). Further, no additional superlattice Bragg reflections in the electron diffraction patterns were observed suggesting that these defects are random and not ordered.

To confirm the presence of the expected elements (Pb, Sb and Se) and the homogeneous single phase nature of the prepared nanocrystals, STEM mode using a 1 nm scanning probe and EDS analysis were used to record elemental maps for all samples. Figure 5a,b shows EDS spectra taken from $Pb_{2.06}Sb_2Se_{5.06}$ nanocrystal. Elemental maps generated based on EDS show that Pb, Sb, and Se are evenly distributed in the lattice further confirming the solid solution behavior (Figure 5c–e). Similar results were obtained for all the nanocrystal compositions, supporting the idea that the nanocrystals prepared through this route are homogeneous solid solutions rather than a phase segregated collection of binary nanophases of PbSe and Sb_2Se_3.

The synthesized $Pb_mSb_{2n}Se_{m+3n}$ nanocrystal aggregates exhibit well-defined band gaps in the mid-IR region. Prior to band gap measurements, capping ligands were removed to prevent the onset of absorption signal from getting swamped. The band gap onset values are around 0.27 eV for all the prepared compositions suggesting that it is independent of the compositions shown in Figure 6. The band gaps of the samples are independent of the composition similar to the previously reported Te analogues. The reason could lie in the fact that the introduction of Sb in the rock-salt lattice introduces orbitals of similar energies to Pb. The band gap values are similar to bulk PbSe.[58] We note that because these are new compounds, there is no corresponding bulk $Pb_mSb_{2n}Se_{m+3n}$ counterparts to compare them with. These band gaps are consistent since the size of the nanocrystal aggregates exceeds the Bohr radius of PbSe (46 nm),[58] so quantum confinement effects may be weak. On the other hand, PbSe nanocrystals synthesized using the same reaction conditions show quantum confinement effects with band gap (~0.35 eV). The bulk band gaps of the individual binary end members are 0.26 and 1.15 eV[41] for PbSe and Sb_2Se_3, respectively.

The thermal stability of the prepared $Pb_mSb_{2n}Se_{m+3n}$ nanocrystal aggregates was assessed by annealing the samples at 400 °C for 4h. The results show that they exhibit moderate stability as exemplified by the $Pb_{2.06}Sb_2Se_{5.06}$ composition which shows complete phase separation into PbSe and Sb_2Se_3 (and Sb_2O_3) when annealed at 400 °C (Figure 7). The presence of Sb_2O_3 is due either to the partial oxidation of the samples or to the incomplete removal of the capping ligand OA prior to the annealing studies. Differential thermal analysis further confirms this phase separation as indicated by the exothermic peak around 385 °C (Figure 7, inset). The exothermic decomposition implies a metastable nature of these compositions on the nanoscale. This is a significantly higher conversion temperature compared to that of the $Pb_mSb_{2n}Te_{m+3n}$ nano-

DOI: 10.1021/jacs.5b05562
J. Am. Chem. Soc. 2015, 137, 9937–9942

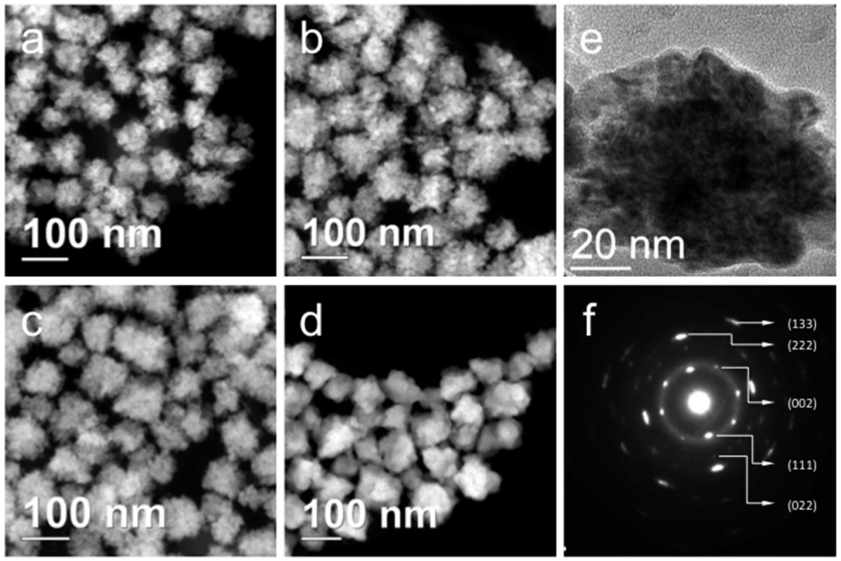

Figure 4. TEM images of as-synthesized (a) $Pb_{2.06}Sb_2Se_{5.06}$, (b) $Pb_{4.08}Sb_2Se_{7.08}$, (c) $Pb_{5.80}Sb_2Se_{8.80}$, and (d) $Pb_{7.66}Sb_2Se_{10.66}$ nanocrystal aggregates. (e) TEM image of an individual $Pb_{2.06}Sb_2Se_{5.06}$ nanocrystal aggregate, showing the aggregation of smaller particles to form the flower-like morphology. (f) SAED pattern from a ~200 × 200 nm area of a grid loaded with nanocrystals. The Bragg reflections show diffuse diffraction spots that can be indexed to the cubic $Fm\bar{3}m$ space group. The diffuse diffraction spots indicates some degree of preferential orientation.

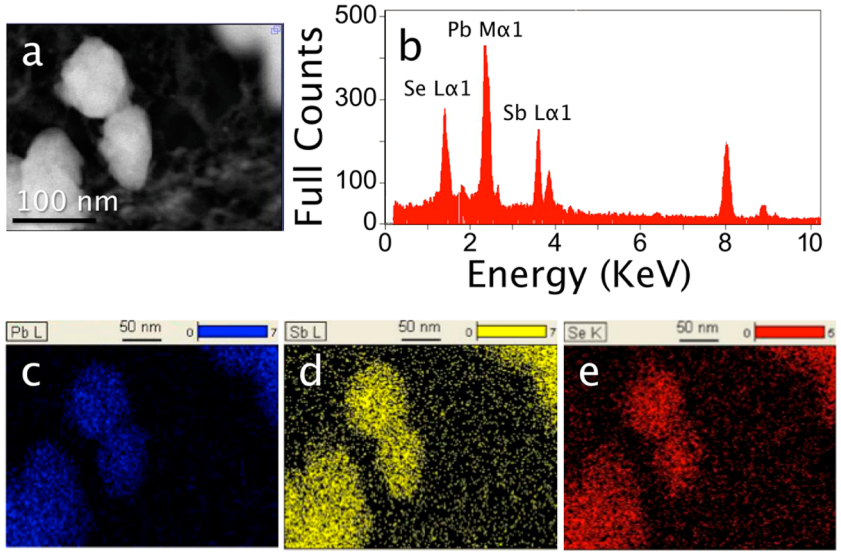

Figure 5. (a) STEM image of $Pb_{2.06}Sb_2Se_{5.06}$ nanocrystal aggregates and (b) the corresponding EDS spectrum showing the presence of all the expected elements in a single nanoparticle. STEM/EDS elemental maps of (c) Pb, (d) Sb, and (e) Se generated from the on EDS analysis.

crystals (~337 °C).[42] Size could very well play a key parameter in accessing these phases which maybe kinetically stabilized above a given size but thermodynamically stabilized below that size.

■ CONCLUSIONS

The pursuit of phases that exists only on the nanoscale and not in the bulk is a relatively unexplored area in nanoparticle science. The novel $Pb_mSb_{2n}Se_{m+3n}$ nanocrystal phases with no corresponding bulk counterparts were prepared using the well-established hot injection method in a one-pot and moderate temperature fashion. The nanocrystal aggregates were comprised of smaller single crystallites that tend to aggregate at a preferred aligned orientation. The aggregates exhibit a moderate monodispersity and well-defined band gaps in the mid-IR region. These nanomaterials are solid solutions with Pb and Sb atoms randomly distributed on the Na sites of the NaCl structure with a presumed large number of metal vacancies due to the 3+ formal charge of Sb in the structure. The new materials tend to phase separate exothermically at a high temperature of 385 °C into the binary PbSe and Sb_2Se_3 end members. They are new phases stabilized only on the nanoscale. The fact that size can be used as a parameter to control composition and crystal structure (as opposed to only electronic structure as predominantly done to date) points to a little explored direction in nanocrystal science and can lead to new materials (with no bulk counterparts). These phases can also aid in our understanding of thermodynamic versus kinetic stability in the nanoscale opening a path to future theoretical studies.

DOI: 10.1021/jacs.5b05562
J. Am. Chem. Soc. 2015, 137, 9937−9942

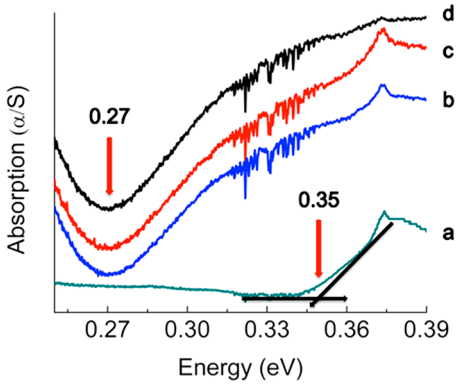

Figure 6. Band gap measurements of (a) PbSe, (b) $Pb_{5.80}Sb_2Se_{8.80}$, (c) $Pb_{4.08}Sb_2Se_{7.08}$, and (d) $Pb_{2.06}Sb_2Se_{5.06}$ nanocrystals using infrared absorption. The band gap of the prepared PbSe nanocrystals (0.35 eV) synthesized using the same conditions is in contrast larger. All samples were stripped of OA capping ligands by stirring in 0.5 M hydrazine in acetonitrile for 2 days and vacuum drying.

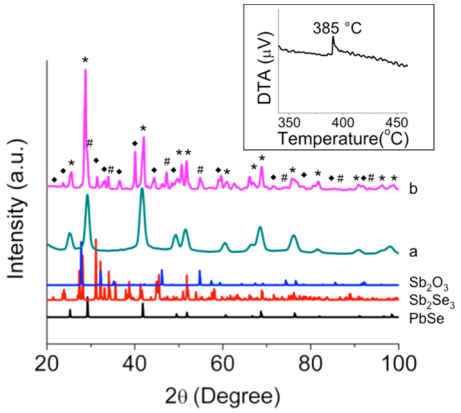

Figure 7. PXRD patterns of $Pb_{2.06}Sb_2Se_{5.06}$ nanocrystals (a) as-synthesized and (b) annealed at 400 °C for 4 h. Diffractions peaks of b are marked with *,◆, and # corresponding to the binary phases PbSe, Sb_2Se_3, and Sb_2O_3, respectively. Simulated PXRD patterns of PbSe (ICSD 74334), Sb_2Se_3 (ICSD 171569), and Sb_2O_3 (ICSD 240206) shown in black, red, and blue lines, respectively. Inset: Differential thermogram showing an exothermic peak around 385 °C which corresponds to the temperature at which phase separation happens.

■ ASSOCIATED CONTENT

Supporting Information

Experimental section (materials, synthesis of $Pb_mSb_{2n}Se_{m+3n}$ nanocrystals, and characterizations), transmission electron micrographs, and elemental composition measurements. The Supporting Information is available free of charge on the ACS Publications website at DOI: 10.1021/jacs.5b05562.

■ AUTHOR INFORMATION

Corresponding Author

*m-kanatzidis@northwestern.edu

Notes

The authors declare no competing financial interest.

■ ACKNOWLEDGMENTS

R.B. Soriano is partly supported by the Hierarchical Materials Cluster Program Fellowship at Northwestern University. We thank the National Science Foundation for partial support of this work via grant DMR-1410169. Electron microscopy and elemental analyses were performed at the Electron Probe Instrumentation Center (EPIC) facility of Northwestern University Atomic and Nanoscale Characterization Experimental (NUANCE) Center (supported by NSF-NSEC, NSF-MRSEC, KECK Foundation, and the State of Illinois) at Northwestern University.

■ REFERENCES

(1) Alivisatos, A. P. *Science* **1996**, *271*, 933.
(2) Nirmal, M.; Norris, D. J.; Kuno, M.; Bawendi, M. G.; Efros, A. L.; Rosen, M. *Phys. Rev. Lett.* **1995**, *75*, 3728.
(3) El-Sayed, M. A. *Acc. Chem. Res.* **2004**, *37*, 326.
(4) Parak, W. J. *Science* **2011**, *334*, 1359.
(5) Schaak, R. E.; Williams, M. E. *ACS Nano* **2012**, *6*, 8492.
(6) Ibáñez, M.; Zamani, R.; Li, W.; Shavel, A.; Arbiol, J.; Morante, J. R.; Cabot, A. *Cryst. Growth Des.* **2012**, *12*, 1085.
(7) Kovalenko, M. V.; Manna, L.; Cabot, A.; Hens, Z.; Talapin, D. V.; Kagan, C. R.; Klimov, V. I.; Rogach, A. L.; Reiss, P.; Milliron, D. J.; Guyot-Sionnnest, P.; Konstantatos, G.; Parak, W. J.; Hyeon, T.; Korgel, B. A.; Murray, C. B.; Heiss, W. *ACS Nano* **2015**, *9*, 1012.
(8) Rogach, A. L.; Eychmuller, A.; Hickey, S. G.; Kershaw, S. V. *Small* **2007**, *3*, 536.
(9) Rogach, A.; Kershaw, S. V.; Burt, M.; Harrison, M. T.; Kornowski, A.; Eychmüller, A.; Weller, H. *Adv. Mater.* **1999**, *11*, 552.
(10) Chen, O.; Zhao, J.; Chauhan, V. P.; Cui, J.; Wong, C.; Harris, D. K.; Wei, H.; Han, H.-S.; Fukumura, D.; Jain, R. K.; Bawendi, M. G. *Nat. Mater.* **2013**, *12*, 445.
(11) Shirasaki, Y.; Supran, G. J.; Bawendi, M. G.; Bulovic, V. *Nat. Photonics* **2012**, *7*, 13.
(12) Kwak, J.; Bae, W. K.; Lee, D.; Park, I.; Lim, J.; Park, M.; Cho, H.; Woo, H.; Yoon, D. Y.; Char, K.; Lee, S.; Lee, C. *Nano Lett.* **2012**, *12*, 2362.
(13) Nazzal, A. Y.; Qu, L.; Peng, X.; Xiao, M. *Nano Lett.* **2003**, *3*, 819.
(14) Talapin, D. V.; Rogach, A. L.; Kornowski, A.; Haase, M.; Weller, H. *Nano Lett.* **2001**, *1*, 207.
(15) Rodriguez-Canto, P. J.; Abargues, R.; Gordillo, H.; Suarez, I.; Chirvony, V.; Albert, S.; Martinez-Pastor, J. *RSC Adv.* **2015**, *5*, 19874.
(16) Konstantatos, G.; Howard, I.; Fischer, A.; Hoogland, S.; Clifford, J.; Klem, E.; Levina, L.; Sargent, E. H. *Nature* **2006**, *442*, 180.
(17) Konstantatos, G.; Sargent, E. H. *Nat. Nanotechnol.* **2010**, *5*, 391.
(18) Lhuillier, E.; Keuleyan, S.; Liu, H.; Guyot-Sionnest, P. *Chem. Mater.* **2013**, *25*, 1272.
(19) Schaller, R. D.; Klimov, V. I. *Phys. Rev. Lett.* **2004**, *92*, 186601.
(20) Luther, J. M.; Beard, M. C.; Song, Q.; Law, M.; Ellingson, R. J.; Nozik, A. J. *Nano Lett.* **2007**, *7*, 1779.
(21) Schaller, R. D.; Sykora, M.; Pietryga, J. M.; Klimov, V. I. *Nano Lett.* **2006**, *6*, 424.
(22) Suryawanshi, M. P.; Agawane, G. L.; Bhosale, S. M.; Shin, S. W.; Patil, P. S.; Kim, J. H.; Moholkar, A. V. *Mater. Technol.* **2013**, *28*, 98.
(23) Dresselhaus, M. S.; Chen, G.; Tang, M. Y.; Yang, R. G.; Lee, H.; Wang, D. Z.; Ren, Z. F.; Fleurial, J. P.; Gogna, P. *Adv. Mater.* **2007**, *19*, 1043.
(24) (a) Talapin, D. V.; Lee, J.-S.; Kovalenko, M. V.; Shevchenko, E. V. *Chem. Rev.* **2010**, *110*, 389. (b) Ibanez, M.; Korkosz, R. J.; Luo, Z.; Riba, P.; Cadavid, D.; Ortega, S.; Cabot, A.; Kanatzidis, M. G. *J. Am. Chem. Soc.* **2015**, *137*, 4046.
(25) Zhang, H.; Son, J. S.; Jang, J.; Lee, J.-S.; Ong, W.-L.; Malen, J. A.; Talapin, D. V. *ACS Nano* **2013**, *7*, 10296.
(26) Fan, F.-J.; Wu, L.; Yu, S.-H. *Energy Environ. Sci.* **2014**, *7*, 190.
(27) Hines, M. A.; Scholes, G. D. *Adv. Mater.* **2003**, *15*, 1844.
(28) Murphy, J. E.; Beard, M. C.; Norman, A. G.; Ahrenkiel, S. P.; Johnson, J. C.; Yu, P.; Micic, O. I.; Ellingson, R. J.; Nozik, A. J. *J. Am. Chem. Soc.* **2006**, *128*, 3241.
(29) (a) Urban, J. J.; Talapin, D. V.; Shevchenko, E. V.; Murray, C. B. *J. Am. Chem. Soc.* **2006**, *128*, 3248. (b) Bozin, E. S.; Malliakas, C. D.; Souvatzis, P.; Proffen, T.; Spaldin, N. A.; Kanatzidis, M. G.; Billinge, S. J. L. *Science* **2010**, *330* (6011), 1660.
(30) Wise, F. W. *Acc. Chem. Res.* **2000**, *33*, 773.

DOI: 10.1021/jacs.5b05562
J. Am. Chem. Soc. 2015, 137, 9937−9942

(31) Murray, C. B.; Sun, S.; Gaschler, W.; Doyle, H.; Betley, T. A.; Kagan, C. R. *IBM J. Res. Dev.* **2001**, *45*, 47.
(32) Fu, H.; Luan, W.; Tu, S.-T. *Dalton Trans.* **2012**, *41*, 12254.
(33) Yang, Z.; Wang, M.; Shi, Y.; Song, X.; Lin, Z.; Ren, Z.; Bai, J. *J. Mater. Chem.* **2012**, *22*, 21009.
(34) Schaller, R. D.; Agranovich, V. M.; Klimov, V. I. *Nat. Phys.* **2005**, *1*, 189.
(35) Procarione, W.; Wood, C. *Phys. Status Solidi B* **1970**, *42*, 871.
(36) Jin, R.; Chen, G.; Pei, J.; Sun, J.; Wang, Y. *Nanoscale* **2011**, *3*, 3893.
(37) Yang, R. B.; Bachmann, J.; Pippel, E.; Berger, A.; Woltersdorf, J.; Gösele, U.; Nielsch, K. *Adv. Mater.* **2009**, *21*, 3170.
(38) Rajpure, K. Y.; Lokhande, C. D.; Bhosale, C. H. *Mater. Res. Bull.* **1999**, *34*, 1079.
(39) Platakis, N. S.; Gatos, H. C. *Phys. Status Solidi A* **1972**, *13*, K1.
(40) Ma, J.; Wang, Y.; Wang, Y.; Chen, Q.; Lian, J.; Zheng, W. *J. Phys. Chem. C* **2009**, *113*, 13588.
(41) Yu, Y.; Wang, R. H.; Chen, Q.; Peng, L. M. *J. Phys. Chem. B* **2006**, *110*, 13415.
(42) Soriano, R. B.; Arachchige, I. U.; Malliakas, C. D.; Wu, J.; Kanatzidis, M. G. *J. Am. Chem. Soc.* **2013**, *135*, 768.
(43) Buck, M. R.; Biacchi, A. J.; Schaak, R. E. *Chem. Mater.* **2014**, *26*, 1492.
(44) Bau, J. A.; Li, P.; Marenco, A. J.; Trudel, S.; Olsen, B. C.; Luber, E. J.; Buriak, J. M. *Chem. Mater.* **2014**, *26*, 4796.
(45) Bergerud, A.; Buonsanti, R.; Jordan-Sweet, J. L.; Milliron, D. J. *Chem. Mater.* **2013**, *25*, 3172.
(46) Vasquez, Y.; Luo, Z.; Schaak, R. E. *J. Am. Chem. Soc.* **2008**, *130*, 11866.
(47) Bondi, J. F.; Misra, R.; Ke, X.; Sines, I. T.; Schiffer, P.; Schaak, R. E. *Chem. Mater.* **2010**, *22*, 3988.
(48) Arachchige, I. U.; Wu, J.; Dravid, V. P.; Kanatzidis, M. G. *Adv. Mater.* **2008**, *20*, 3638.
(49) Zhao, Y.; Dyck, J. S.; Hernandez, B. M.; Burda, C. *J. Am. Chem. Soc.* **2010**, *132*, 4982.
(50) (a) Arachchige, I. U.; Kanatzidis, M. G. *Nano Lett.* **2009**, *9*, 1583. Karkamkar, A. J.; Kanatzidis, M. G. *J. Am. Chem. Soc.* **2006**, *128*, 6002.
(51) Wang, D.; Zheng, W.; Hao, C.; Peng, Q.; Li, Y. *Chem. Commun.* **2008**, 2556.
(52) Hu, J.; Lu, Q.; Tang, K.; Qian, Y.; Zhou, G.; Liu, X. *Chem. Commun.* **1999**, *12*, 1093.
(53) Steinhagen, C.; Panthani, M. G.; Akhavan, V.; Goodfellow, B.; Koo, B.; Korgel, B. A. *J. Am. Chem. Soc.* **2009**, *131*, 12554.
(54) Khare, A.; Wills, A. W.; Ammerman, L. M.; Norris, D. J.; Aydil, E. S. *Chem. Commun.* **2011**, *47*, 11721.
(55) Shavel, A.; Arbiol, J.; Cabot, A. *J. Am. Chem. Soc.* **2010**, *132*, 4514.
(56) Elagina, E. I. *Vopr. Metall. Fiz. Poluprovodn.* **1963**, *4*, 119.
(57) Houtepen, A. J.; Koole, R.; Vanmaekelbergh, D.; Meeldijk, J.; Hickey, S. G. *J. Am. Chem. Soc.* **2006**, *128*, 6792.
(58) Joo, J.; Pietryga, J. M.; McGuire, J. A.; Jeon, S.-H.; Williams, D. J.; Wang, H.-L.; Klimov, V. I. *J. Am. Chem. Soc.* **2009**, *131*, 10620.

DOI: 10.1021/jacs.5b05562
J. Am. Chem. Soc. 2015, 137, 9937−9942